# Calculated properties of fully hydrogenated single layers of BN, $BC_2N$, and graphene: Graphane and its BN-containing analogues

Frank W. Averill,[1,2] James R. Morris,[1,2] and Valentino R. Cooper[1]
[1]*Materials Science and Technology Division, Oak Ridge National Laboratory, Oak Ridge, Tennessee 37831, USA*
[2]*Department of Materials Science and Engineering, University of Tennessee, Knoxville, Tennessee 37996-0750, USA*
(Received 19 August 2009; revised manuscript received 13 October 2009; published 16 November 2009)

Carbon is an attractive material for hydrogen adsorption due to its light weight, variety of structures, and ability to both physisorb and chemisorb hydrogen. Recently, fully hydrogenated graphene layers ("graphane") have been predicted to exist [J. O. Sofo *et al.*, Phys. Rev. B **75**, 15340 (2007)], and experimentally observed [D. C. Elias *et al.*, Science **323**, 610 (2009)]. In this work, we examine analogs of graphane, in particular $BNH_2$ and $BC_2NH_4$. Unlike graphene, these materials have a band gap without hydrogenation. Our results indicate that the hydrogenation product of BN is metastable: the fully hydrogenated compound $BNH_2$ is higher in energy than hexagonal BN sheets plus $H_2$ molecules, in sharp contrast with graphane. We find that $BC_2NH_4$ is energetically very close to hexagonal $BC_2N+2H_2$ molecules. Furthermore, our examination of the relative binding strengths of rows of symmetry related hydrogen atoms on $BC_2NH_4$ shows that this compound is marginally higher in energy than $BC_2NH_2$ plus an $H_2$ molecule, with the hydrogen atoms in $BC_2NH_2$ absorbed on the carbon sites. These remaining hydrogen atoms are not as strongly bound as in graphane, indicating that the average hydrogen chemisorption energy is controllable by changing the carbon content in the B-C-N layer.

DOI: 10.1103/PhysRevB.80.195411 PACS number(s): 61.48.De, 62.23.Kn, 68.43.Fg, 81.05.Uw

## I. INTRODUCTION

The chemical and structural similarities of graphite and the hexagonal layered forms of boron nitride (*h*-BN) and boron di-carbon nitride have long intrigued chemists and physicists.[1] All these systems are layered materials composed of strongly bonded $sp^2$ hybridized atoms but where the layers are mostly bound by van der Waals forces. Although, graphite and *h*-BN are isoelectronic, their properties differ due to the partial ionic nature of the B–N bond. For instance, graphite is an electrical conductor (or a semi-metal) whereas boron nitride is a large band gap semiconductor. Behaviors expressed in these materials have resulted in the investigation and exploitation of these materials and their single-layered forms for a number of modern applications. For example, the conductivity of graphite has led to the exploration of carbon-based materials for electrochemical energy storage.[2] The well known ability of carbon, *h*-BN and related materials to absorb various molecules[3] makes them favorable for numerous possible applications such as Li-intercalated anodes[4] and hydrogen storage.[5–11] Recent experiment and theory also point to the possible use of graphene nanopores for molecular and ionic sieves.[12,13]

The recent isolation of individual sheets of graphite (graphene)[14] has generated much research activity, particularly with regards to understanding how the electronic properties of individual sheets may be tuned by controlling the dimensions of the sheets. Another avenue of inquiry has been to explore chemically modified graphene and similar materials,[15] especially with chemisorbed hydrogen atoms on individual sheets[16,17] and fully hydrogenated graphene (graphane).[18,19] The chemisorption of atomic hydrogen on graphene has been predicted to be collective: when the coverage is low, the heat of chemisorption is positive, requiring energy to form;[16,17] however, once there is some adsorption, further adsorption is more favorable, eventually leading to a negative (favorable) average heat of chemisorption. Flat sheets that are only hydrogenated on one side of the graphene sheet have a positive heat of chemisorption, though this may change when the sheet has some curvature.[19] In contrast to the partially occupied case, fully hydrogenated graphane has been predicted to be lower in formation energy than benzene.[18]

The prediction[18] and subsequent observation[19] of graphane, and the similarity in bonding between carbon and boron nitride, lead to the question of the existence and properties of their boron-carbon-nitride analogs BN ("BN-phene"), $BC_2N$ ("$BC_2N$-phene"), and their fully hydrogenated derivatives $BNH_2$ ("BN-phane") and $BC_2NH_4$ ("$BC_2N$-phane"). BN has a zincblende ground state, but also has a metastable hexagonal graphitic equivalent ("white graphite" or *h*-BN). The ability of BN to form graphene-like planes makes these compounds interesting counterparts to their carbon-based structures. Nanotubes of boron nitride have been extensively studied both experimentally and theoretically.[20,21] Still more recently, single sheets of *h*-BN (i.e., BN or BN-phene) have been fabricated[22] and are now receiving new theoretical attention.[23] Although single sheets of BN alone may have many potential applications, we focus on $BNH_2$, its fully hydrogenated derivative. $BNH_2$ has not yet been detected in the laboratory and its properties are still largely unknown, unlike graphene, graphane, and single-sheet BN. In particular, the chemisorption of hydrogen on single-sheet BN has not been explored. The fact that a close relative, ammonia-borane ($H_3BNH_3$) is under examination as a possible hydrogen storage medium[23–25] is at the very least encouraging. Carbon–hydrogen bonds are generally stronger than B–H or N–H bonds (and generally considered too strong for reversible hydrogen storage), making the relative stability of "BN-phane" an open question.

The addition of carbon to boron nitride compounds has often been used to alter or "tune" the properties of BN for a

 

particular application. One example is the addition of carbon to BN to reduce the band gap into the visible light region.[25,26] Although B-N-C materials have a tendency to segregate into BN and C,[27,28] experimental evidence exists for some relatively stable $BC_xN$ materials.[26,28] Among these, $BC_2N$ seems particularly robust.[26,28] In this article, we shall focus our efforts on understanding the properties of the fully hydrogenated compound, $BC_2NH_4$, as well as fully hydrogenated BN and graphene sheets. Although investigations of the physisorption of molecular hydrogen in $BC_2N$ nanotubes have been carried out,[29] the authors are not aware of any work on fully hydrogenated monolayers of $BC_2N$, particularly for chemisorbed hydrogen.

In this work, we theoretically examine the possible existence of two B-N-C containing analogs of graphane: hydrogenated single sheets of hexagonal boron nitride ($BNH_2$ or "BN-phane") and those of boron di-carbon nitride ($BC_2NH_4$ or "$BC_2N$-phane"). In particular, we determine their relative formation energies, their physical and electronic structure, and the strength of their X–H bonds. After summarizing our numerical and theoretical methods in Sec. II, we present BN-phene and $BC_2N$-phene results in Sec. III followed by those of BN-phane and $BC_2N$-phane in Sec. IV A summary and conclusions are given in Sec. V

## II. METHODS

The computations were carried out using density functional theory[30,31] as implemented in the plane-wave based Vienna *ab initio* Simulation Package (VASP) (Ref. 32) and the projector augmented wave (PAW) method.[33] Exchange and correlation energies were approximated by the semilocal generalized gradient approximation (GGA) of Perdew, Burke, and Ernzerhof (PBE).[34]

In order to accommodate the three-dimensional periodicity requirements of plane-wave basis sets, single layered systems (like graphene and graphane) were infinitely replicated in the $z$ direction with adjacent layers separated by at least 9 Å in order to minimize any spurious interaction between them. Individual atoms and molecules were likewise simulated by three-dimensional arrays of identical atoms and molecules separated by at least 9 Å in all directions. Brillouin zone integration was performed by the Monkhorst-Pack method[35] using an $11\times11\times1$ $k$-point grid for single layered systems and by a single $\Gamma$ $k$ point for atoms and molecules. The plane-wave cutoff was set at 600 eV, where convergence was achieved.

Cohesive energies were computed as the difference in the energy of the system in question and the sum of the isolated atom energies. By this definition, bound systems have negative cohesive energies.

## III. RESULTS: BN AND $BC_2N$ ANALOGUES OF GRAPHENE

The BN and $BC_2N$ lattices are shown in Fig. 1 with the structural parameters for these systems in Table I. Like their all carbon analog graphene, these systems form strong planar hexagonal sheets. In BN, (see Table I) the B–N bond distance of 1.45 Å compares well with the experimental value[36] (also 1.45 Å) for the related solid phase, $h$-BN, and with the C–C bond distance, we (1.43 Å) and Sofo *et al.*[18] (1.42 Å) have computed for graphene. The computed BN cohesive energy of −7.10 eV/atom has a lower magnitude than that of graphene (−7.99 eV/atom) but is still significant and is reflective of the strength and stability of this system. The computed energy band gap (4.66 eV) is in agreement with that computed by Ishigami and co-workers (4.5 eV), but both differ from the experimental value for $h$-BN [37,38] of 5.8 eV. However, the GGA PBE potential is well known to systematically underestimate energy band gaps[39] by as much as 40% so an error of 20% in the band gap is not unexpected. Comparison can also be made with the very recent work of Li *et al.*[23] on BN where they used the same plane-wave code (VASP) but a different exchange-correlation potential [local density approximation (LDA) Ceperley and Alder][40] and obtained a computed B–N bond distance of 1.44 Å and a direct band gap at the $K$ symmetry point of 4.61 eV. State of the art GW band gap calculations on other related BN containing materials[41–43] show significant increases in the band gaps relative to those obtained using GGA PBE. There seems to be little doubt that BN is a large band gap semiconductor.

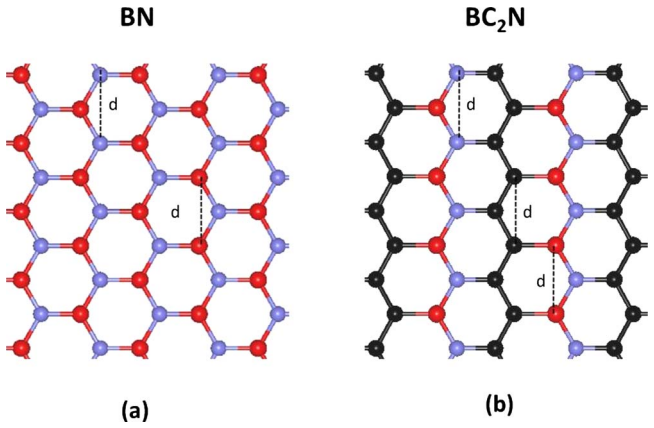


FIG. 1. (Color online) Two-dimensional lattices of (a) BN, and (b) $BC_2N$. In the online color figure, nitrogen atoms are blue, borons are red, and carbons are black. Like graphene, both lattices are flat. The structural parameters for these lattices are given in Table I. It can be seen that this particular conformer of $BC_2N$ can be obtained from BN by replacing every other vertical zigzag row of B-N's with C-C's. Graphene (not shown) has the same hexagonal lattice as these but where all the atoms are carbon. The dotted lines define in-plane lattice constants "$d$" between like atoms.

The atomic arrangement chosen here for $BC_2N$ [see Fig. 1(b)] is the one predicted[44] among fully integrated and nonsegregated alternatives to have the lowest energy. This structure consists of two sets of alternating zigzag chains of C-C atoms and B-N atoms joined together into hexagonal rings by successive B–C and N–C bonds. This structure has been shown to be only metastable relative to segregated BN and graphene,[27] as confirmed by our calculations. If $BC_2N$ segregates into BN and graphene, the result will have a cohesive energy of −7.54 eV/atom, which is 0.23 eV more stable than that of $BC_2N$ (−7.31 eV/atom). The bond distances of the $BC_2N$ nearest neighbors vary between 1.39 Å (N–C) and

TABLE I. Computed structural parameters for graphene, BN-phene, and $BC_2N$-phene. (see Fig. 1 for images of the lattices.) Distances between atoms A-B and in-plane lattice constants between like atoms "*d*" are in Å and angles A-B-C are in degrees where B is the vertex. In-plane lattice constants between like atoms "*d*" are defined in Fig. 1. Cohesive energies per atom (C.E./atom) and energy band gaps (band gap) are in eV.

| | | |
|---|---|---|
| Graphene | | |
| *d* | 2.47 | Å |
| C-C | 1.43 | Å |
| C-C-C | 120.0° | |
| C.E./atom | −7.98 | eV |
| Band gap | 0.00 | eV |
| BN-phene | | |
| *d* | 2.51 | Å |
| B-N | 1.45 | Å |
| B-N-B | 120.0° | |
| N-B-N | 120.0° | |
| C.E./atom | −7.10 | eV |
| Band gap | 4.66 | eV |
| $BC_2N$ | | |
| *d* | 2.50 | Å |
| B-N | 1.45 | Å |
| B-C | 1.52 | Å |
| N-C | 1.39 | Å |
| C-C | 1.43 | Å |
| N-B-N | 119.0° | |
| B-N-C | 120.5° | |
| N-C-C | 118.9° | |
| C-C-C | 122.2° | |
| C.E./atom | −7.31 | eV |
| Band gap | 1.66 | eV |

1.52 Å (B–C). The average bond distance around the two $BC_2N$ inequivalent rings is about 1.44 Å, placing it nicely between that of BN (1.45 Å) and graphene (1.43 Å). The calculated cohesive energy of $BC_2N$ is also roughly between that of BN and graphene, though considerably closer to BN than graphene. $BC_2N$ is computed to be a semiconductor with a band gap of only 1.66 eV. The aforementioned tendency of the GGA PBE potential to under estimate band gaps, leads one to believe that the experimental band gap should be in the range of 2–3 eV.

## IV. RESULTS: $BNH_2$ and $BC_2NH_4$ ANALOGUES OF GRAPHANE: ENERGIES OF FORMATION AND HYDROGENATION

The structures of $BNH_2$ and $BC_2NH_4$ (see Fig. 2 and Table II) are similar to graphane in that both form hexagonal lattices where atom $X$ ($X$=B,N,C) puckers out of the plane

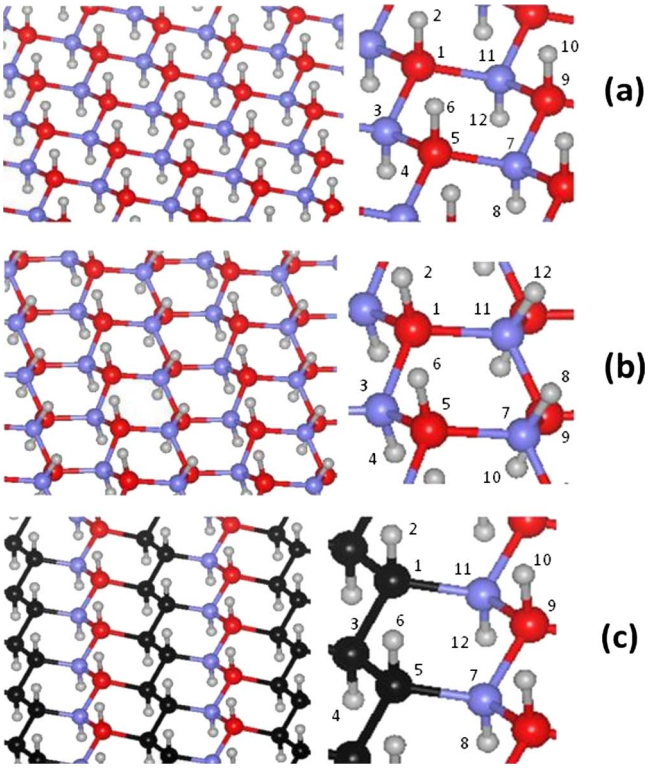


FIG. 2. (Color online) Lattices of (a) $BNH_2$ chair conformer, (b) $BNH_2$ boat conformer, and (c) $BC_2NH_4$ chair. In the online color figure, nitrogen atoms are blue, borons red, carbons black, and hydrogens are gray. The numbers in the hexagonal cells provide the atom identifications used in Tables II and III. Graphane (not shown) has the same hexagonal lattices as these but where boron and nitrogen atoms are replaced by carbon.

toward the hydrogen atom to which it is bound. Like graphane, $BNH_2$ has both chair and boat conformations, but unlike graphane in which the chair conformation is 0.05 eV more stable, the boat and chair conformers of $BNH_2$ have about the same energy (see Table II). Although the search was not exhaustive, no stable boat conformation was found for $BC_2NH_4$. These fully hydrogenated materials are semiconductors with computed chair conformer band gaps of 3.75 eV ($BNH_2$) and 3.43 eV ($BC_2NH_4$) closely bracketing the 3.69 eV band gap of graphane. Like their pure carbon analogs, $BNH_2$ and $BC_2NH_4$ have larger in-plane lattice constants than their unhydrogenated parents although the increase for the boat conformer of $BNH_2$ is quite trivial (0.01 Å).

It should be noted here that while our computed cohesive energies and structural parameters for graphane (see Table IIa) are very similar to those calculated by others,[18,45] they do differ significantly from the calculations of Boukhvalov *et al.*[46] and recent TEM measurements of Elias *et al.*[19] In particular, we find that graphane has a slight in-plane *expansion* relative to graphene: from 2.47 Å for graphene (Table Ia) to 2.54 Å for graphane (Table IIa), while these studies indicate a *contraction* of the in-plane lattice spacing of graphane relative to graphene. Elias[19] measured the lattice constant of graphene to be $2.46 \pm 0.02$ Å, which is in the range of the 2.47 Å value we computed, but they determined the lattice

TABLE II. Computed structural parameters for graphane, BN-phane, and $BC_2N$-phane. Distances between atoms A-B and in-plane lattice constants between like atoms ($d$) are in Å and angles A-B-C in degrees with B being the vertex of the angle. Cohesive energies per atom (C.E./atom), average X–H bond energy per H atom (X-H/H atom), and energy band gaps (band gap) are in eV. The in-plane lattice constant $d$ between like atoms is defined in Fig. 1 and atom location identification numbers are shown in Fig. 2. Although graphane is not specifically shown in Fig. 2, the same atom location identification numbers used for the chair and boat conformers of $BNH_2$ apply. The average X-H/H atom energy is defined in Eq. (2).

| Graphane | Chair | Boat | $BC_2NH_4$ | |
|---|---|---|---|---|
| $d$ | 2.54 Å | 2.52 Å | $d$ | 2.57 Å |
| C1-C3 | 1.54 Å | 1.53 Å | B9-N7 | 1.58 Å |
| C5-C7 | 1.54 Å | 1.58 Å | N7-C5 | 1.50 Å |
| C1-H2 | 1.11 Å | 1.11 Å | C1-C3 | 1.54 Å |
| C1-C3-C5 | 111.5° | 110.2° | B9-H10 | 1.22 Å |
| C3-C5-C7 | 111.5° | 112.8° | N7-H8 | 1.03 Å |
| C1-C3-H4 | 107.4° | 107.2° | C1-H2 | 1.10 Å |
| C.E./atom | −5.23 eV | −5.18 eV | C3-H4 | 1.12 Å |
| X-H/H atom | −2.48 eV | −2.37 eV | B9-N7-C5 | 112.3° |
| Band gap | 3.69 eV | 3.75 eV | N7-B9-N11 | 108.7° |
| | $BNH_2$ | | N7-C5-C3 | 111.2° |
| $d$ | 2.60 Å | 2.52 Å | C1-C3-C5 | 113.1° |
| B1-N3 | 1.59 Å | 1.56 Å | C1-C3-H4 | 107.6° |
| B1-H2 | 1.20 Å | 1.22 Å | C3-C1-H2 | 108.2° |
| N3-H4 | 1.03 Å | 1.03 Å | N7-C5-H6 | 104.4° |
| B1-N3-B5 | 110.0° | 107.9° | C5-N7-H8 | 106.5° |
| N3-B5-N7 | 110.0° | 110.5° | N7-B9-H10 | 107.6° |
| B1-N3-H4 | 108.9° | 107.4° | C.E./atom | −4.83 eV |
| N3-B5-H6 | 108.9° | 109.5° | X-H/H atom | −2.35 eV |
| N7-B5-H6 | 108.9° | 108.8° | Band gap | 3.43 eV |
| C.E./atom | −4.59 eV | −4.60 eV | | |
| X-H/H atom | −2.09 eV | −2.11 eV | | |
| Band gap | 3.75 eV | 5.08 eV | | |

constant of graphane to be smaller than graphene and near to the Boukhvalov value of 2.42 Å. Boukhvalov *et al.*[46] calculated C-C and C-H distances (1.52 and 1.10, respectively) very similar to those of other calculations, including the present work (1.54 and 1.11 Å), but obtained a much smaller C–C–C bond angle (102.8° as compared to 111.5°), which is consistent with the in-plane contraction that they observe. Our larger angle is closer to the ideal tetrahedral angle of 109.5° commonly seen in $sp^3$ bonding and would imply a more complete transition from $sp^2$ bonding in graphene to $sp^3$ in graphane. To test the sensitivity of these particular results to the choice of exchange-correlation potential, we recalculated the lattice constants of graphene and graphane using the LDA potential of Ceperley and Alder[40] as parameterized by Perdew and Zunger.[47] As is typical of LDA, the lattice constants (graphene: 2.45 Å and graphane: 2.51 Å) were smaller than in GGA, but the percentage of expansion of the graphane lattice constant relative to graphene remained about the same as before (LDA: 2.4%, GGA: 2.8%).

From cohesive energies and the computed $H_2$ dissociation energy (−2.28 eV/atom, excluding zero-temperature vibrational energy), it is possible to compute the formation energy for these systems. We define the formation energy of an arbitrary hydrogenated system, $AH_n$, as

$$E_{for} = E^{coh}_{AH_n} - E^{coh}_{A} - n\frac{E^{diss}_{H_2}}{2}, \quad (1)$$

where the quantities $E^{coh}_{AH_n}$ and $E^{coh}_{A}$ are the cohesive energies of the hydrogenated system ($AH_n$) and an unhydrogenated reference system (A) and $E^{diss}_{H_2}$ is the dissociation energy of $H_2$ excluding any vibrational or thermal energies. Formation energies per atom for some C-C, B-N, and B-N-C systems are shown in Fig. 3. Formation energies for the $C_mH_n$ systems in Fig. 3 were previously computed by Sofo *et al.*[18] also using the GGA PBE exchange-correlation energy but with a different set of pseudopotentials (Vanderbilt ultrasoft pseudopotentials)[48] and a different plane-wave code (CASTEP).[49] Although their cohesive energies are systematically much lower than ours and the experimental values, the relative order of their energies are the same and therefore the qualitative picture for these systems remains unchanged. The

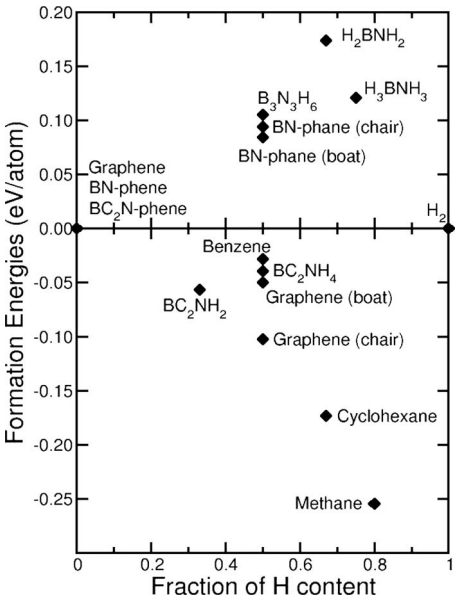


FIG. 3. Formation energies per atom (in eV/atom) of carbon, boron, nitrogen, and hydrogen containing systems as functions of their fractional H content. For $C_mH_n$ systems, the reference parent system along with the free $H_2$ molecule is graphene. For $(BN)_mH_n$ systems, the reference system is BN-phene, and for $BC_2NH_n$ systems, it is $BC_2N$-phene. Formation energy is defined in Eq. (1). The formation energies of the free molecules, aminoborane ($H_2BNH_2$), ammonia-borane ($H_3BNH_3$), borazine ($B_3N_3H_6$), benzene ($C_6H_6$), cyclohexane ($C_6H_{12}$), and methane ($CH_4$) are given for reference. The other systems shown are isolated single sheet materials.

calculated formation energies are sensitive to the cohesive energies of the bulk systems and to the binding energy of $H_2$; our values for both of these are smaller in magnitude than those of Ref. 18. In particular, there is a significant discrepancy in the calculated $H_2$ dissociation energy that contributes significantly to the quantitative difference between our results and those of Sofo *et al.* The dissociation energy of $H_2$ is an exception from most molecules we have investigated, having a computed value that is actually higher rather than lower than the experimental value (−2.38 eV/atom, without zero-temperature vibrational and thermal energies).[50] Nevertheless, as in Ref. 18, our calculations show graphane to be very stable; i.e., lower in formation energy per atom than benzene.

However, the formation energy picture for $(BN)_mH_n$ systems is very different from their carbon analogs. From Fig. 3, it can be seen that $(BN)_mH_n$ systems all have positive formation energies relative to BN-phene and $H_2$ and will be only metastable. Nevertheless, the case has already been made experimentally by Stephens *et al.*[24] that ammonia-borane ($H_3BNH_3$) could be a hydrogen source if an economical means can be found for regeneration. From a purely formation energy viewpoint, BN-phane appears to be nearly as stable as ammonia-borane (see Fig. 3). Aminoborane ($H_2BNH_2$), and borazine ($B_3N_3H_6$) are analogs of ethylene and benzene and their formation energies are given for reference.

The total X–H bond energy in a unit cell can be computed as the difference between the cohesive energy of the hydrogenated system and its corresponding unhydrogenated parent system. The average X–H bond energy per H atom is then obtained by dividing the total X–H bond energy by the number of H atoms in the cell. Therefore, the average X–H bond energy per H atom of an arbitrary hydrogenated system $AH_n$ introduced in Eq. (1) would be

$$E_{av}^{\text{X-H bond}} = 1/n(\text{E}_{\text{AH}_n}^{\text{coh}} - \text{E}_{\text{A}}^{\text{coh}}). \quad (2)$$

Note that the total energy of the isolated hydrogen atom is included through the calculation of the cohesive energy, and therefore is accounted for in the calculation of the bond energy. The values for $BC_2NH_4$ (−2.35 eV) and $BNH_2$ (−2.09 eV-chair, −2.11 eV-boat) shown in Table II can be compared to the (−2.48 eV-chair, −2.37 eV-boat) values for graphane. For the lowest energy conformers, the calculated average X–H bond energies per H atom fall in the order of graphane (−2.48 eV) < $BC_2NH_4$(−2.35 eV) < $BNH_2$(−2.11 eV). Interestingly, the calculated dissociation energy of $H_2$ is −2.28 eV/H atom, which, once again, along with the formation energies in Fig. 3, points to the relative ease with which $BNH_2$ is likely to give up hydrogen. The addition of carbon to BN clearly leads to an increase in the average strength of X–H bonds and hints at the possibility of using carbon content as a way of managing that strength in individual layers of $(BN)_mC_n$ materials.

Whereas the *average* strength of binding of hydrogen atoms increases with carbon content, the *individual* strengths of the B–H, C–H, and N–H bonds need to be examined as well. To assess the individual strengths of the four symmetry inequivalent X–H bonds in $BC_2NH_4$ [see Fig. 2(c)], periodic rows of H were removed and the resulting $BC_2NH_3$ lattices were allowed to relax. From the cohesive energies of these relaxed systems, the strengths of the four X–H bonds were computed as the difference in the cohesive energies of the original system $AH_n$ and the cohesive energy of the system with all symmetry equivalent hydrogen atoms removed from atom X; i.e.,

$$E^{\text{X-H bond}} = \text{E}_{\text{AH}_n}^{\text{coh}} - \text{E}_{\text{AH}_{n-1}}^{\text{coh}}. \quad (3)$$

These four values are shown in Table IIIa.III The bond strength of the N–H bond is seen to be the weakest, which is consistent with N being saturated by just three single bonds and therefore more than willing to give up one of its four. Of course, if additional hydrogen atoms are removed, the X–H bond energies change and will depend upon the order in which hydrogen atoms are removed. To illustrate, all four rows of hydrogen atoms were removed first in the order of H8 (and H12) from the nitrogen atoms, H10 from the boron atoms, H2 (and H6) from the C1 (and C5) carbon atoms, and H4 from the C4 carbon atoms [see Fig. 2(c) and Table IIIb] resulting successively in the systems $BC_2NH_3$, $BC_2NH_2$, $BC_2NH$, and $BC_2N$. The computed bond energies were, respectively, −3.99, −0.54, −4.23, and −0.66 eV. The average of these bond energies is −2.35 eV, which corresponds to the value given for the average H bond energy in $BC_2NH_4$ in Table IIc. This demonstrates that removing the hydrogen atom from the nitrogen (breaking the weakest bond) dramati-

TABLE III. (a) X–H bond energies per hydrogen atom as one of the four inequivalent hydrogens is removed from $BC_2NH_4$ forming $BC_2NH_3$. See Fig. 2(c) for definitions of atom reference numbers. The X–H bond energies are defined in Eq. (3). There are two inequivalent carbon atoms in the unit cell: carbons atoms 1 and 5 are nearest neighbors to N's where as carbon 3 has B as a nearest neighbor. (b) The X–H bond energies per hydrogen atom as rows of hydrogen atoms are successively removed in the order of (i) H8 (also H12), (ii) H10, (iii) H2 (also H6), and (iv) H4 resulting first in $BC_2NH_3$ then $BC_2NH_2$, $BC_2NH_1$, and finally $BC_2N$. (c) The successive X–H bond energies as rows of hydrogen atoms are removed in order of (i) H8 (also H12), (ii) H2 (also H6), (iii) H4, and (iv) H10. Note that regardless of the order of removal, the average of the four successive X–H bond energies is always 2.35 eV, which is the average X–H bond energy per H atom of $BC_2NH_4$ (see Table IIc). In rows (b) and (c) of the Table, the roman numbers i–iv indicate the order in which rows of inequivalent hydrogen atoms are removed. All bond energies are in eV.

| | N7-H8, N11-H12 | B9-H10 | C1-H2, C5-H6 | C3-H4 |
|---|---|---|---|---|
| (a) | −3.99 | −4.53 | −4.53 | −4.45 |
| (b) | −3.99(i) | −0.54 (ii) | −4.23(iii) | −0.66(iv) |
| (c) | −3.99(i) | −0.73(iv) | −1.36 (ii) | −3.34(iii) |

cally affects the B–H bond. Similarly, breaking one C–H bond weakens the other. This is similar to the collective binding observed in graphane.

In another illustration of collective binding, if $BC_2N$-phane ($BC_2NH_4$) has hydrogen atoms removed from the nitrogens, the resulting $BC_2NH_3$ system has a +0.20 eV/atom formation energy (see Fig. 3) making it metastable relative to an equivalent mixture of $BC_2NH_4$ and $BC_2NH_2$. If now the weakly bound H atoms are also removed from B atoms, the new $BC_2NH_2$ system has a formation energy that is surprisingly 0.26 eV/atom lower at −0.06 eV/atom. As can be seen from Fig. 3, this conformer of $BC_2NH_2$ binds its remaining hydrogen atoms as strongly to its carbon atoms as graphane. In Fig. 4, side views of these three layered systems, $BC_2NH_4$, $BC_2NH_2$, and $BC_2NH_2$, are shown along with some representative bond distances. It can be seen that removing hydrogen atoms from the nitrogen atoms of $BC_2NH_4$ and forming $BC_2NH_3$ [Fig. 4(b)] strengthens the B–N bonds (i.e., decreases the bond distance) but at the expense of weakening the boron bonds to hydrogen and carbon. Removing the hydrogen atoms from boron to form highly stable $BC_2NH_2$ [Fig. 4(c)] puts each atom in its optimal coordination. This last material may be viewed as being formed of alternating zigzag chains of BN-phene and graphane.

The internal consistency of the computed X–H bond energies is supported by their confirmation of Hess's Law: if the order of hydrogen removal is changed (For example, as in Table IIIc), the individual bond energies change but the average stays the same. In principle, there are $4!=24$ ways in which to remove the four inequivalent hydrogen atoms from $BC_2NH_4$ and we have not attempted to evaluate them all. However, some general observations can be made: the first row of hydrogen atoms appears to be the most difficult to remove but the last comes off relatively easily although

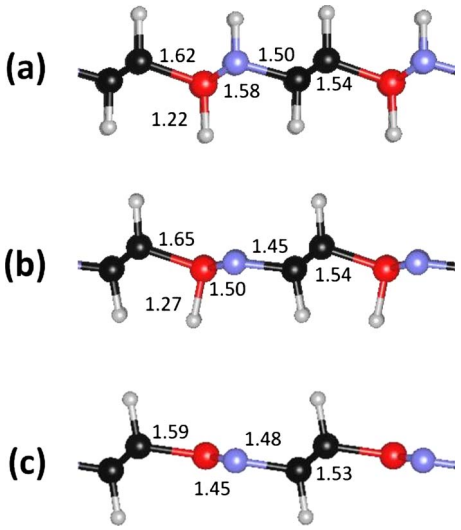


FIG. 4. (Color online) Side views of single sheets of (a) $BC_2N$-phane; i.e., $BC_2NH_4$, (b) the conformer of $BC_2NH_3$, formed from $BC_2NH_4$ by removing hydrogen atoms bound to nitrogen atoms and (c) the conformer of $BC_2NH_2$ formed from the aforementioned $BC_2NH_3$ by removing hydrogen atoms bound to boron atoms. In the online color figure, nitrogen atoms are blue, borons red, carbons black, and hydrogens are gray. Numbers in the figure are computed bond distances in Å.

there may be rows of hydrogen atoms between the first and the last that come off even easier as in Table IIIb.

The full hydrogenation of graphene to graphane (see Table II) increases the computed band gap regardless of the conformer of graphane: from zero to 3.69 eV for the chair, and from zero to 3.75 eV for the boat. Hydrogenation of BN is distinctly different, with the band gap already at 4.66 eV in BN: the gap increases in the boat conformer of $BNH_2$ to 5.08 eV, but decreases in the chair to 3.75 eV. As has been seen by others,[26] the addition of carbon to BN decreases its band gap: in this work from 4.66 eV for BN to 1.66 eV for $BC_2N$. When $BC_2N$ is then hydrogenated to form $BC_2NH_4$ chair, the band gap is again increased from 1.66 to 3.43 eV, but still falls somewhat short of the 3.69 eV value found for the graphane chair.

## V. SUMMARY AND CONCLUSION

In an effort to assess their stability and electronic properties, two hypothetical graphane analogs, $BNH_2$ and $BC_2NH_4$, and their unhydrogenated parent compounds BN and $BC_2N$ were investigated using density functional theory (DFT). We find that, like graphene and hexagonal BN, the structure of the BN-based hydrogenated materials is quite similar to that of graphane yet all three compounds (graphane, BN-phane and $BC_2N$-phane) exhibit significant differences in relative stabilities and electronic structures. With regards to structural similarities, our results indicate that the hydrogenation of both graphene (to make graphane) and the BN based analogs results in a slight *expansion* in the in-plane lattice parameters as the bonds between the B, N, and C species change character from purely $sp^2$ (in the parent compounds) to tetrahe-

dral or $sp^3$ (in the hydrogenated materials). We note that while these results are consistent with previous work,[18,45] they contradict recent TEM measurements of Elias *et al.*[19] and theoretical studies of Boukhvalov *et al.*[46] We observe that the computed bond lengths of our calculations and those of Boukhvalov and Katsnelson[51] are comparable and that the discrepancy in lattice parameters stems from deviations in the C–C–C bond angles.

Our comparison of the relative stability and electronic structure of the three isoelectronic, hydrogenated materials reveals three main points. First, we find that the relative stability of the hydrogenated material is enhanced with increasing carbon content. Here, graphane was determined to be the most stable compound, i.e., forming the strongest bonds with adsorbed H, while $BNH_2$ would prefer to dissociate into $BN+H_2$. In the case of $BC_2N$, which is energetically metastable relative to segregated BN-phene and graphene, the hydrogenated compound $BC_2NH_4$ is lower in energy than the separate $BC_2N$-phene and isolated $H_2$. Remarkably, $BC_2NH_4$ was computed to bind hydrogen atoms as strongly as benzene. Furthermore, we find the binding of H to $BC_2N$ to be cooperative as in the case of graphene. Our results indicate that in $BC_2NH_4$, H atoms bind weakest to N atoms and that the removal of these H atoms forming $BC_2NH_3$ dramatically weakens B–H bonds but has little effect on the remaining, strong C–H bonds. As a result, removing the hydrogen atoms from the boron and nitrogen sites and forming $H_2$ molecules and $BC_2NH_2$ dramatically lowers the formation energy, indicating that this conformer of $BC_2NH_3$ is only metastable. The remaining hydrogens bound to the carbon sites still require a significant energy to desorb, larger than that required to break the N–H bonds of the original $BC_2NH_4$ compound.

A second observation is the disparity between the ground-state structures of the hydrogenated, carbon containing compounds and $BNH_2$. Here, we find that for both graphane and $BC_2NH_4$ the chair confirmation is the preferred structure, while $BNH_2$ has nearly degenerate chair and boat conformers. Again, for $BNH_2$ neither boat nor chair is stable relative to dissociation into $BN+H_2$. Also, although the search was not exhaustive, no stable boat conformer of $BC_2NH_4$ was found: starting structures either released hydrogen or relaxed to the chair conformation. These results certainly suggest that either the boat conformer is unstable, or is marginally stable relative to the chair conformation.

A third consequence of hydrogenation is the observed trends in the computed band gaps. Despite the fact that the three parent compounds have significantly different band gaps, which narrow upon increasing carbon content (i.e., BN has a relatively large band gap of 4.66 eV, graphene is a semimetal with no band gap and $BC_2N$ has a band gap that lies between the two end members, 1.66 eV) the three hydrogenated materials have surprisingly similar band gaps (3.69, 3.75, 3.43, and 3.75 eV for graphane chair, graphane boat, $BC_2NH_4$ and $BNH_2$ chair, respectively). The major difference is that for the carbon containing compounds, hydrogenation raises band gaps while for BN it lowers the gap of the chair conformer but raises that of the boat. We speculate that this is because the electronic states determining the band gap are now related to the X–H bonding interactions.

In conclusion, our calculations demonstrate that many of the properties of B-N-C hexagonal layered materials may be tuned by controlling the carbon content of the sheet. This is indicative of the sensitivity of materials properties to their detailed composition, even among these isoelectronic compounds. These results hint at the possibility of using the addition of carbon to BN as a way of increasing the average X–H bond strength in $(BN)_mH_n$ materials; thereby possibly stabilizing compounds that would ordinarily segregate into BN and carbon.

## ACKNOWLEDGMENTS

The authors would like to thank C. Contescu and C. L. Fu for useful comments on the manuscript. J.R.M. would like to thank Peter Tortorelli for bringing Ref. 19 to his attention. The authors acknowledge support by the Division of Materials Sciences and Engineering, the U. S. Department of Energy under Contract No. DE-AC0500OR22725 with UT–Battelle, LLC. This research used resources of the National Energy Research Scientific Computing Center, which is supported by the Office of Science of the U.S. Department of Energy under Contract No. DE-AC02-05CH11231. Lattice plots made using VESTA software.[52]

[1] L. Pauling, Proc. Natl. Acad. Sci. U.S.A. **56**, 1646 (1966).
[2] E. Frackowiak and F. Beguin, Carbon **39**, 937 (2001).
[3] Adsorption by Carbons, in edited by E. J. Bottani and J. M. D. Tascon (Elsevier Science, Oxford, England, 2008).
[4] W. B. Xing, J. S. Xue, T. Zheng, A. Gibaud, and J. R. Dahn, J. Electrochem. Soc. **143**, 3482 (1996).
[5] V. V. Bhat, C. I. Contescu, and N. C. Gallego, Nanotechnology **20**, 204011 (2009).
[6] M. Ishigami, J. D. Sau, S. Aloni, M. L. Cohen, and A. Zettl, Phys. Rev. Lett. **97**, 176804 (2006).
[7] R. S. Aga, C. L. Fu, M. Krcmar, and J. R. Morris, Phys. Rev. B **76**, 165404 (2007).
[8] M. Jordá-Beneyto, F. Suárez-García, D. Lozano-Castelló, D. Cazorla-Amorós, and A. Linares-Solano, Carbon **45**, 293 (2007).
[9] S. Patchkovskii, J. S. Tse, S. N. Yurchenko, L. Zhechkov, T. Heine, and G. Seifert, Proc. Natl. Acad. Sci. U.S.A. **102**, 10439 (2005).
[10] W. Q. Deng, X. Xu, and W. A. Goddard, Phys. Rev. Lett. **92**, 166103 (2004).
[11] S. H. Jhi, Phys. Rev. B **74**, 155424 (2006).
[12] K. Sint, B. Wang, and P. Král, J. Am. Chem. Soc. **130**, 16448 (2008).
[13] D. E. Jiang, V. R. Cooper, and S. Dai, Nano Lett. (to be published).
[14] K. S. Novoselov, A. K. Geim, S. V. Morozov, D. Jiang, Y. Zhang, S. V. Dubonos, I. V. Grigorieva, and A. A. Firsov, Science **306**, 666 (2004).

[15] R. Ruoff, Nat. Nanotechnol. **3**, 10 (2008).
[16] D. Stojkovic, P. Zhang, P. E. Lammert, and V. H. Crespi, Phys. Rev. B **68**, 195406 (2003).
[17] Y. Lin, F. Ding, and B. I. Yakobson, Phys. Rev. B **78**, 041402 (2008).
[18] J. O. Sofo, A. S. Chaudhari, and G. D. Barber, Phys. Rev. B **75**, 153401 (2007).
[19] D. C. Elias, R. R. Nair, T. M. G. Mohiuddin, S. V. Morozov, P. Blake, M. P. Halsall, A. C. Ferrari, D. W. Boukhvalov, M. I. Katsnelson, A. K. Geim, and K. S. Novoselov, Science **323**, 610 (2009).
[20] C. Y. Zhi, Y. Bando, C. C. Tang, Q. Huang, and D. Golberg, J. Mater. Chem. **18**, 3900 (2008).
[21] D. Golberg, Y. Bando, C. C. Tang, and C. Y. Zhi, Adv. Mater. **19**, 2413 (2007).
[22] K. S. Novoselov, D. Jiang, F. Schedin, T. J. Booth, V. V. Khotkevich, S. V. Morozov, and A. K. Geim, Proc. Natl. Acad. Sci. U.S.A. **102**, 10451 (2005).
[23] J. Li, G. Gui, and J. X. Zhong, J. Appl. Phys. **104**, 094311 (2008).
[24] F. H. Stephens, V. Pons, and R. T. Baker, Dalton Trans. **2007**, 2613 (2007).
[25] M. T. Nguyen, V. S. Nguyen, M. H. Matus, G. Gopakumar, and D. A. Dixon, J. Phys. Chem. A **111**, 679 (2007).
[26] M. O. Watanabe, S. Itoh, T. Sasaki, and K. Mizushima, Phys. Rev. Lett. **77**, 187 (1996).
[27] K. Yuge, Phys. Rev. B **79**, 144109 (2009).
[28] X. G. Luo, Z. Y. Liu, J. L. He, B. Xu, D. L. Yu, H. T. Wang, and Y. J. Tian, J. Appl. Phys. **105**, 043509 (2009).
[29] J. Rossato, R. J. Baierle, T. M. Schmidt, and A. Fazzio, Phys. Rev. B **77**, 035129 (2008).
[30] P. Hohenberg and W. Kohn, Phys. Rev. **136**, B864 (1964).
[31] W. Kohn and L. J. Sham, Phys. Rev. **140**, A1133 (1965).
[32] G. Kresse and J. Furthmuller, Comput. Mater. Sci. **6**, 15 (1996).
[33] G. Kresse and D. Joubert, Phys. Rev. B **59**, 1758 (1999).
[34] J. P. Perdew, K. Burke, and M. Ernzerhof, Phys. Rev. Lett. **77**, 3865 (1996).
[35] H. J. Monkhorst and J. D. Pack, Phys. Rev. B **13**, 5188 (1976).
[36] E. K. Sichel, R. E. Miller, M. S. Abrahams, and C. J. Buiocchi, Phys. Rev. B **13**, 4607 (1976).
[37] A. Zunger, A. Katzir, and A. Halperin, Phys. Rev. B **13**, 5560 (1976).
[38] M. Ishigami, S. Aloni, and A. Zettl, in *12th International Conference on Scanning Tunneling Microscopy/Spectroscopy and Related Techniques*, edited by P. M. Koenraad and M. Kemerink, AIP Conf. Proc. No. 696 (AIP, New York, 2003), p. 94.
[39] J. Heyd and G. E. Scuseria, J. Chem. Phys. **121**, 1187 (2004).
[40] D. M. Ceperley and B. J. Alder, Phys. Rev. Lett. **45**, 566 (1980).
[41] L. Wirtz, A. Marini, and A. Rubio, Phys. Rev. Lett. **96**, 126104 (2006).
[42] C. H. Park, C. D. Spataru, and S. G. Louie, Phys. Rev. Lett. **96**, 126105 (2006).
[43] B. Arnaud, S. Lebegue, P. Rabiller, and M. Alouani, Phys. Rev. Lett. **96**, 026402 (2006).
[44] A. Y. Liu, R. M. Wentzcovitch, and M. L. Cohen, Phys. Rev. B **39**, 1760 (1989).
[45] S. Casolo, O. M. Lovvik, R. Martinazzo, and G. F. Tantardini, J. Chem. Phys. **130**, 054704 (2009).
[46] D. W. Boukhvalov, M. I. Katsnelson, and A. I. Lichtenstein, Phys. Rev. B **77**, 035427 (2008).
[47] J. P. Perdew and A. Zunger, Phys. Rev. B **23**, 5048 (1981).
[48] D. Vanderbilt, Phys. Rev. B **41**, 7892 (1990).
[49] M. D. Segall, P. J. D. Lindan, M. J. Probert, C. J. Pickard, P. J. Hasnip, S. J. Clark, and M. C. Payne, J. Phys.: Condens. Matter **14**, 2717 (2002).
[50] W. E. Dasent, *Inorganic Energetics: An Introduction* (Cambridge University Press, Cambridge, England, 1982).
[51] D. W. Boukhvalov and M. I. Katsnelson, Nano Lett. **8**, 4373 (2008).
[52] K. Momma and F. Izumi, J. Appl. Crystallogr. **41**, 653 (2008).